Experimental Evaluation of Radar Waveforms for Spectral Coexistence using the PARSAX radar

Carotenuto, V.; Aubry, A.; De Maio, A.; Fioranelli, F.; Krasnov, O.; Yarovoy, A.; van der Zwan, W.F.

DOI
10.1109/MetroAeroSpace57412.2023.10190037

Publication date
2023

Document Version
Final published version

Published in
Proceedings of the 2023 IEEE 10th International Workshop on Metrology for AeroSpace (MetroAeroSpace)

Experimental Evaluation of Radar Waveforms for Spectral Coexistence using the PARSAX radar

V. Carotenuto, A. Aubry, A. De Maio
DIETI, University of Naples "Federico II"
via Claudio 21, Naples, Italy
{vincenzo.carotenuto, augusto.aubry, ademaio}@unina.it

F. Fioranelli, O. Krasnov, A. Yarovoy, and F. van der Zwan
MS3 Group, Department of Microelectronics, TU Delft
Mekelweg 4, 2628CD Delft, The Netherlands
{f.fioranelli, o.a.krasnov, a.yarovoy, w.f.vanderzwan}@tudelft.nl

2023 IEEE 10th International Workshop on Metrology for AeroSpace (MetroAeroSpace) | 978-1-6654-5690-6/23/$31.00 ©2023 IEEE | DOI: 10.1109/METROAEROSPACE57412.2023.10190037

***Abstract*—This paper investigates the possibility of transmitting waveforms designed to enable spectral coexistence between radar and other Radio Frequency (RF) wireless systems via a Software Defined Radar (SDR). The design technique tested in this study nominally enables the placement of notches in the spectrum of the synthesized probing radar signal. Their widths and depths are set during the design stage so as to accounting for the interference into each shared frequency interval, allowing for spectral coexistence. At the assessment stage, the synthesized signal is used with the PARSAX radar system, an SDR capable of operating in the S frequency band. The analysis first focuses on studying the compliance of the signal generated by the PARSAX radar with its theoretical counterpart. Subsequently, open-air experiments are conducted in the presence of stationary and moving targets. The results show that the spectral characteristics of the probing radar signal adhere well to the theoretical spectral mask, and prove the system ability to detect both stationary and moving targets.**

***Index Terms*—Cognitive Radar, Spectral Coexistence, Waveform Design, Software Defined Radar.**

I. Introduction

Spectral cohabitation among radar and wireless emitters operating within the same frequency band has gained significant attention during the last decade, as also testified by the number of published research [1]–[26]. The problem arises because the growth of high data-rate wireless communication services has led to a crowded and crowded of the Radio Frequency (RF) spectrum, especially in some frequency bands of particular interest for radar applications. As a consequence, the radar has to effectively capitalize on the available spectral resources, while avoiding to interfere with other overlaid frequency emitters. However, while it is important to ensure spectral coexistence, it is equally important to guarantee satisfactory detection, estimation, and tracking performance to the radar system.

To reach this goal, in [6] a waveform design technique has been proposed enabling spectral coexistence while optimizing the radar Signal-to-Interference plus Noise Ratio (SINR). This is obtained by placing bespoke notches in the spectrum of the synthesized waveform in order to provide a precise control on the amount of interference injected by the radar in each shared frequency interval (in the following referred to as 'stop bands'). Additionally, this technique also allows to control some features of the radar probing waveform which, on the whole, rule the radar performance. The practical implementation of the technique has already been studied in [27] and [28] by using a hardware-in-the-loop testbed, also accounting for possible distortions induced on the probing signal by Power Amplifiers (PAs). However, for the final validation of the waveform generation strategy, the spectrally-notched signal has to be transmitted in open-air, and both spectral coexistence and radar performance have to be assessed.

Given the outlined context, the aim of this paper is to investigate the feasibility of transmitting the waveforms designed according to the algorithm proposed in [6] through a Software Defined Radar (SDR). Precisely, the designed signal is used as input to the PARSAX radar system, an S-band SDR located on the roof of the EEMCS (Electrical Engineering, Mathematics & Computer Science) faculty at TU Delft, in Delft, The Netherlands, and operated by the Microwave Sensing, Signals & Systems (MS3) research group. The radar gives the possibility of transmitting customized digital waveforms generated via an Arbitrary Waveform Generator (AWG). Leveraging this capability, this study is firstly focused on assessing the compliance between the signal produced by the PARSAX and the waveform designed to ensure spectral coexistence exploiting a feedback channel available in the SDR system. Then, experiments are carried out by transmitting the probing signal in open-air considering different scenarios encompassing the presence of stationary and moving targets. The results demonstrate that the spectral characteristics of the probing signal conform to the theoretical spectral mask, while the system is able to detect both stationary and moving targets.

The remainder of this paper is organized as follows. In Section II, the measurement setup is described. In Section III the results of the experimental analysis are discussed. Finally, in Section IV conclusions are drawn and possible future research avenues are pointed out.

II. Measurement Setup

The PARSAX radar [29] shown in Figure 1 as already pointed out has been used for the experiments presented in this paper. The system is located on the roof of the EEMCS faculty at TU Delft, in Delft, The Netherlands. PARSAX is a highly reconfigurable, medium-range S-band SDR operated in its conventional use as Frequency Modulated Continuous

978-1-6654-5690-6/23/$31.00 ©2023 IEEE

Wave (FMCW) radar. It is capable of operating in a fully-polarimetric mode, with two independent polarimetric channels both in transmission and reception and at high resolution, with bandwidth up to 100 MHz and resulting range resolution up to 1.5m.

The radar has high sensitivity, with transmitted continuous power up to +50 dBm per channel and receiver noise floor around -93 dBm; this allows to detect target signatures up to distances of a few tenths of kilometers, depending on their Radar Cross Section (RCS). To prevent the saturation of the receiver circuits by the too strong reflected signal from the nearest objects, the transmit power can be set in two modes according to the radar task: (a) high power mode (+50 dBm), used for atmospheric observation, and (b) lower power mode (+23 dBm), used for ground-based targets observation.

The PARSAX radar is designed as a SDR with digital signal processing implementation up to the intermediate frequency of 125 MHz. It includes a fully reprogrammable 4-channel AWG that can generate signals based on the sequence of prerecorded waveform samples with the rate of 1.2 GSample/sec. These real-valued samples have to represent the probing waveform at the intermediate frequency of 125 MHz with the maximum bandwidth of ± 50 MHz. The generated waveform is passed to the analog circuits of the transmitter to be up-converted to RF with a carrier of 3.315 GHz. Then, it is amplified and radiated towards the search direction via the transmit antenna. A copy of this signal is also exploited in the reference channel of the digital receiver for customized signal processing.

Within the receiver board, the received and reference signals are synchronously sampled via parallel ADCs with a sampling rate of 400 MHz in a 14 bits digital representation. Further, these sampled signals are sent to the FPGA for joint signal processing. Depending on the type of sensing waveforms, different radar signal receiver designs can be loaded in the FPGA for real-time operation [30]. This can include a different version of the Linear Frequency Modulated (LFM) signals' de-ramping receiver (with real and complex mixers, low-pass filters, with and without range compression), frequency-based implementation of the matched filter receiver of arbitrary signals, or direct streaming receiver that simply transfers the sampled signal to the computer for further processing. The main characteristics of the PARSAX radar are summarized in Table I.

Fig. 1: The TU Delft PARSAX radar, located on the roof of the EEMCS Faculty and operated by the MS3 group.

TABLE I: Main characteristics of the PARSAX radar [31].

Category	Parameter	Value
System characteristics	Center frequency	3.315 GHz
	Modulation bandwidth	$\leq$ 100 MHz
	Range resolution	$\leq$ 1.5 m
Power characteristics	Max. power per channel	100/0.2 W
	Transmitter attenuation	$\leq$ 80 dB
Transmitter parabolic antenna	Antenna diameter	4.28 m
	Antenna beamwidth	1.8°
	Antenna gain	40.0 dBi
Receiver parabolic antenna	Antenna diameter	2.12 m
	Antenna beamwidth	4.6°
	Antenna gain	32.8 dB
TX-RX isolation	HH-polarized	-100 dB
	VV-polarized	-85 dB
ADC characteristics	Max. sampling frequency	400 MHz
	ADC resolution	14-bit
	Spur-free dynamic range	$\geq$ 70 dB

For the experimental results of this paper, the radar has been operated in single polarization mode, specifically with horizontal polarization in both transmission and reception, and in low power mode to avoid saturation of the receiver channel, i.e., transmitting +23 dBm. Raw radar data have been collected, amounting to approximately 1.6 GByte/s by sampling both the transmitted and received channels. This corresponds to 400 MSamples/s for the transmitted signal and for the received signal, where each sample occupies 14 bits, i.e. 2 bytes.

One notable characteristic of the PARSAX radar is the possibility to use customized, digitally generated waveforms in transmission thanks to the usage of an AWG, with the additional possibility of setting up FPGA-based programmable processing also at the receiver side. In the experiments reported in this study, customized signals have been only adopted in transmission using the AWG to generate waveforms designed according to the algorithm in [6]. Hence, data have been collected in two scenarios as detailed in the following.

A. *Scenario 1: single target of opportunity*

The radar has been pointed toward a stationary target of opportunity located at approximately 1.14 km. This target is a tall chimney, made of four co-located cylindrical pipes as in Figure 2.

B. *Scenario 2: multiple moving targets of opportunity*

The radar has been pointed toward an highway segment located at approximately 4.02 km, as shown in the maps of Figure 3. This scenario allows to test the radar performance in the presence of multiple moving targets of opportunity, i.e., uncooperative vehicles driving in both directions of the highway.

III. Experimental Analysis

This section first focuses on describing the characteristics of the waveform used in the experimental analysis. Subsequently,

the results obtained by sensing the environment with the synthesized signal are discussed.

A. Waveform Design

The waveform used for the experimental analysis is designed according to the algorithm proposed in [6]. It enables the cohabitation between radar and wireless systems operating in the same frequency band by tailored notching the spectrum of the radar signal in correspondence of the desired stop bands. The design parameters are the individual width and depth of each notch and a similarity-like constraint. The latter allows to control some relevant features of the radar probing signal, such as variations in the signal modulus as well as Integrated Sidelobe Level (ISL) and Peak-to-Sidelobe Level (PSL).

For the experiments in this study, the reference signal is a LFM waveform with a duration of 50 μs and a bandwidth equal to 40 MHz. As to the spectral coexistence scenario, it is supposed the presence of three emitters operating over the spectral intervals $[f_i^l, f_i^u]$, $f_i^u - f_i^l = 2$ MHz, $i = 1, \ldots, 3$. Additionally, an interference level of -35 dB in each stop band is guaranteed.

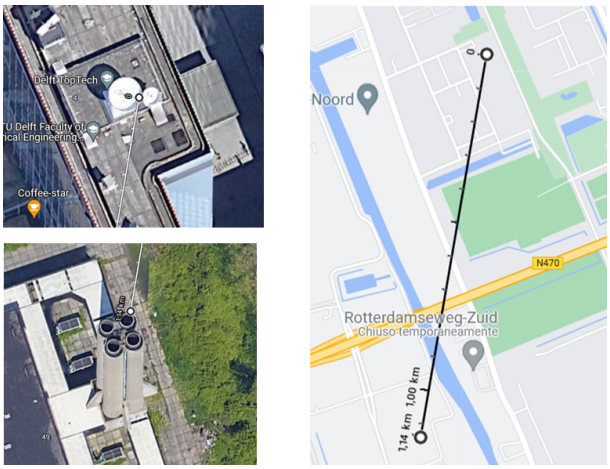

Fig. 2: Scenario 1 with a stationary target of opportunity: chimney.

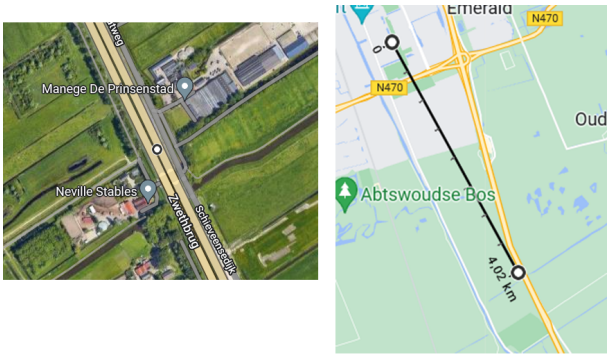

Fig. 3: Scenario 2 with multiple targets of opportunity: moving vehicles on a highway segment.

After the waveform synthesis, bursts of uniformly time-spaced pulses are formed using a pulse repetition time of 200 μs. Finally, for both scenarios outlined in Section II, the burst is transmitted via the PARSAX and the signals backscattered from the environment are collected and analyzed considering a coherent processing interval composed of 512 pulses. Table II summarizes the main parameters involved in the experimental analysis.

Parameter	Value
Pulse Width	50 μs
Bandwidth	40 MHz
Pulse repetition time	200 μs
Number of processed pulses	512
Number of stop bands	3
Stop-bands width	2 MHz
Notches depth	-35 dB

TABLE II: Parameters involved in the experimental analysis.

Before discussing the results, it is worth pointing out that the PARSAX system uses two distinct antennas for simultaneous transmission and reception, thus enabling short-range detection with no blind range. Hence, detecting targets within the considered scenarios using the specified pulse parameters is not an issue.

B. Results and discussion

The first analysis is aimed at verifying the similarity between the synthesized waveform (denoted in the following as 'theoretical signal') and the signal generated by the AWG of the PARSAX. This initial assessment is crucial because possible hardware imperfections in the AWG may introduce spectral distortions in the produced waveform, potentially compromising the spectral compatibility requirement. The comparison is provided in both time and frequency domain in Figure 4. Specifically, Figure 4(a) and 4(b) show the real parts and the frequency spectral densities of the theoretical and generated signal (note that for both the analyses the curves are normalized with respect to their maximum value).

The comparison reveals a good agreement between the two waveform. Moreover, a linear attenuation of the generated signal during the pulse duration is clearly visible in both the time and frequency domains. This attenuation only affects the amplitude of the generated signal and can be compensated with a suitable pre-calibration of the AWG.

The next analysis focuses on determining whether the hardware components downstream the AWG in the transmit chain of the PARSAX system (such as mixers, filters, and amplifiers, among others) compromise the spectral compatibility of the signal being transmitted in the open air. This study is conducted using the signals backscattered from the environment of Scenario 1, which mainly involves a chimney located at a relatively short-range. Given the narrow beam of the transmit antenna and the high RCS of the chimney, and as a consequence the high SINR, it is expected that the received signals are just a delayed copies of the probing waveform, with a time elapse proportional to the range of the target. The results of this assessment are displayed in Figures 5(a) and 5(c)

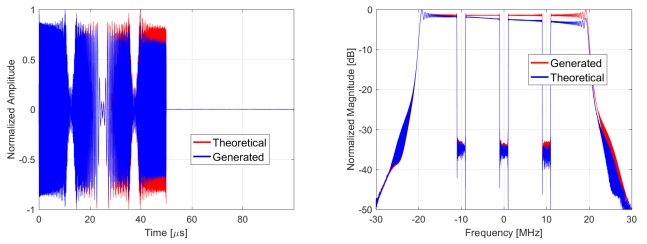

(a) (b)

Fig. 4: Comparison between theoretical and experimentally generated signals in time domain (a) frequency domain (b).

in both time and frequency domains, respectively. Figure 5(a) shows the real-part of the signals collected from Scenario 1 during a CPI (composed of 512 pulses). Figure 5(c) compares the frequency spectral densities of the theoretical, generated, and received signals, with the curves for the received signals obtained by averaging the frequency spectra evaluated using all 512 pulses in the CPI.

The analysis in the time-domain in Figure 4(a) confirms that the received signals can be viewed as delayed versions of the transmitted waveform, with the delay matching the range of the chimney. The frequency spectrum curves show that the depth of the frequency notches remains almost unchanged, indicating that the probing signal transmitted in open air satisfies the spectral constraints set during the design stage. However, a spurious contribution at -25 MHz is clearly visible in the frequency spectrum of the received signal. It is difficult to determine whether this is due to the transmit or receive circuits of the PARSAX as the processed signal experiences both the chains. Further assessments will be conducted to investigate this aspect in the future.

The same analysis is carried on for Scenario 2 and the results are displayed in Figures 5(b) and 5(d). As outlined in Section II, this scenario involves multiple moving targets on a highway located approximately 4 km away from the radar. This is reflected in the more complex structure of the signals received during the CPI, as shown in Figure 5(b), compared with those collected for Scenario 1. Nonetheless, Figure 5(d) indicates that the depth of the frequency notches in the stop-bands still complies with the spectral constraints set to ensure the compatibility between the probing waveform transmitted in open air and the external electromagnetic environment.

Finally, Figures 6 and 7 show the range profiles and the range-Doppler maps obtained using the signals received for both the analyzed scenarios during a CPI. The range profile in Figure 6(a) and the range-Doppler map in Figure 7(a) for Scenario 1 exhibit a peak located at the range of the chimney and at zero-Doppler, as expected due to the stationary nature of the target. On the other hand, the range profile in Figure 6(b) for Scenario 2 displays a more intricate shape than in the former case, suggesting the presence of multiple targets. This is confirmed by the corresponding range-Doppler map in Figure 7(b) which reveals the presence of multiple scatters

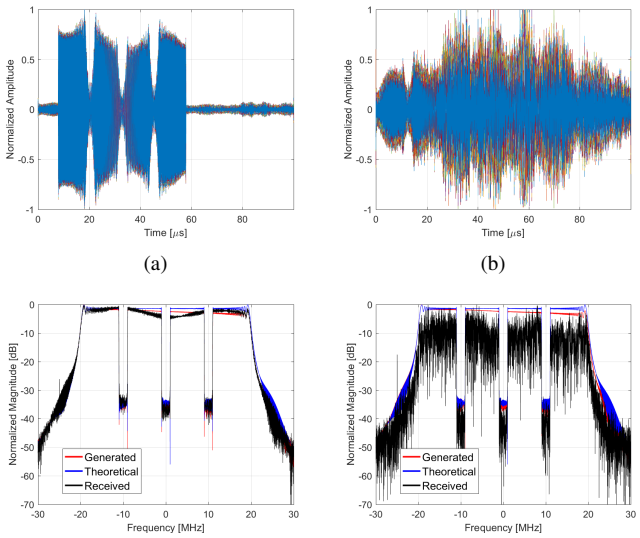

(a) (b)

(c) (d)

Fig. 5: Time/frequency domain behaviour of the signals collected for Scenario 1 (a), (c), and Scenario 2 (b), (d).

moving towards and away from the radar, with velocities and ranges consistent with the highway segment illuminated by the radar.

Summarizing, the obtained results reveal that for both scenarios the waveform generated by the AWG and the probing radar signal transmitted in open-air comply with the spectral requirements set at the design stage to ensure spectral co-existence. Furthermore, the range profiles and range-Doppler maps demonstrate the capability of the system to detect both stationary and moving targets via the designed spectrally-notched waveform.

IV. Conclusions

This paper has presented an experimental validation on the transmission in an open-air environment of spectrally-notched waveforms enabling RF frequency bandwidth sharing among radar and overlaid wireless emitters. Specifically, the probing radar signal has been designed according to the technique proposed in [6] and used to feed the PARSAX system, an SDR equipped with an AWG and capable of operating in the S frequency band. After describing both the main features of the system and the scenarios considered for the experimental validation, different analyses have been conducted. The first assessment has been focused on verifying the compliance of the waveform generated by the AWG as well as the probing signal transmitted in open-air with their theoretical counterpart. Then, the detection capability of the system has been investigated in the presence of both stationary and moving targets.

The results have highlighted a good agreement between the spectral features of the waveform generated by the AWG and the waveform transmitted in open-air with the theoretical spectral mask forced at the design stage to ensure spectral

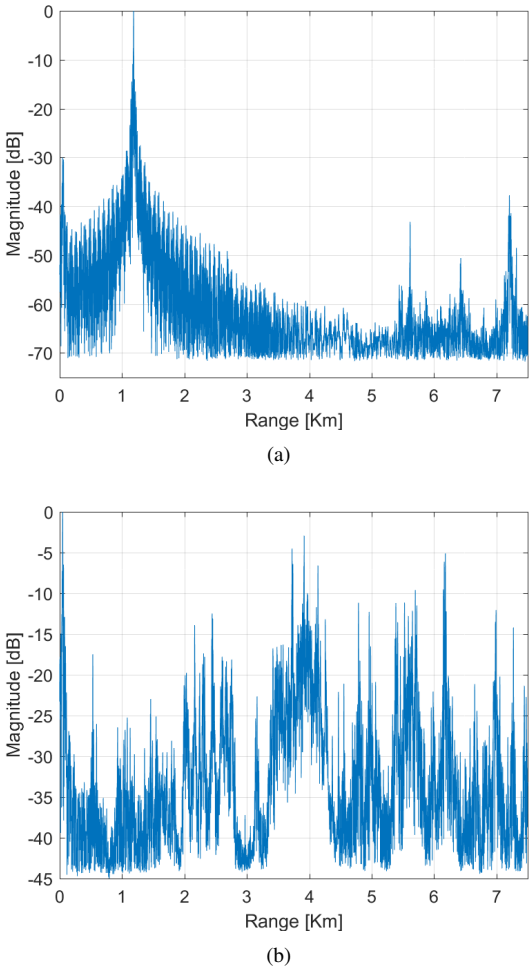

Fig. 6: Range profile after pulse compression applying non-coherent integration for scenario 1 (a), and scenario 2 (b).

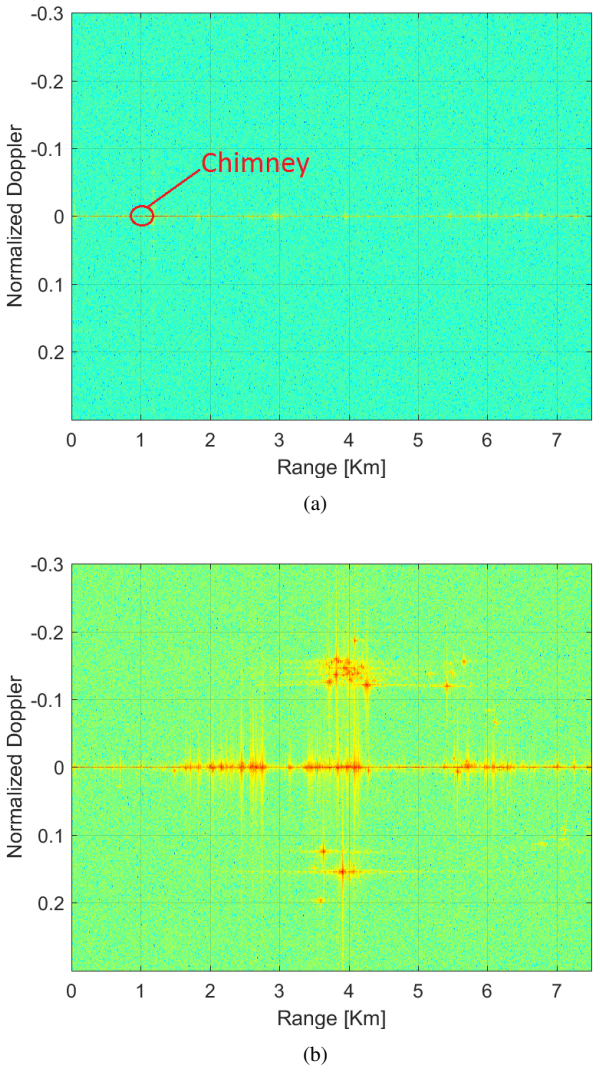

Fig. 7: Range-Doppler maps for scenario 1 with stationary target of opportunity (a) and scenario 2 with multiple moving targets (b).

coexistence. Additionally, for both scenarios considered in the experimental campaigns, the obtained range profiles and range-Doppler maps have highlighted that by using the designed spectrally-notched waveform, the system is able to detect both stationary and moving targets.

Future research directions might focus on investigating the source of the spurious contribution observed in the frequency spectrum of the received signals, as well as exploring the transmission of waveforms designed according to other spectral constraints.

Acknowledgements

The work of V. Carotenuto was supported by the research program PON R&I AIM1878982-1. The work of A. Aubry and A. De Maio was partially supported by the European Union under the Italian National Recovery and Resilience Plan (NRRP) of NextGenerationEU, partnership on "Telecommunications of the Future" (CUP J33C22002880001, PE00000001 - program RESTART).

References

[1] H. Griffiths, L. Cohen, S. Watts, E. Mokole, C. Baker, M. Wicks, and S. Blunt, "Radar Spectrum Engineering and Management: Technical and Regulatory Issues," *Proceedings of the IEEE*, vol. 103, no. 1, pp. 85–102, 2015.

[2] H. Griffiths, "Where has all the Spectrum Gone?" in *2013 International Conference on Radar*, 2013, pp. 1–5.

[3] B. Paul, A. R. Chiriyath, and D. W. Bliss, "Survey of RF Communications and Sensing Convergence Research," *IEEE Access*, vol. 5, pp. 252–270, 2017.

[4] L. Zheng, M. Lops, Y. C. Eldar, and X. Wang, "Radar and Communication Coexistence: An Overview: A Review of Recent Methods," *IEEE Signal Processing Magazine*, vol. 36, no. 5, pp. 85–99, 2019.

[5] A. Aubry, V. Carotenuto, A. De Maio, A. Farina, and L. Pallotta, "Optimization Theory-based Radar Waveform Design for Spectrally Dense Environments," *IEEE Aerospace and Electronic Systems Magazine*, vol. 31, no. 12, pp. 14–25, 2016.

[6] A. Aubry, V. Carotenuto, and A. D. Maio, "Forcing Multiple Spectral Compatibility Constraints in Radar Waveforms," *IEEE Signal Processing Letters*, vol. 23, no. 4, pp. 483–487, 2016.

[7] A. Aubry, A. De Maio, M. A. Govoni, and L. Martino, "On the Design of Multi-Spectrally Constrained Constant Modulus Radar Signals," *IEEE Transactions on Signal Processing*, vol. 68, pp. 2231–2243, 2020.
[8] B. Tang and J. Liang, "Efficient Algorithms for Synthesizing Probing Waveforms with Desired Spectral Shapes," *IEEE Transactions on Aerospace and Electronic Systems*, vol. 55, no. 3, pp. 1174–1189, 2019.
[9] S. D. Blunt, M. Cook, J. Jakabosky, J. De Graaf, and E. Perrins, "Polyphase-Coded FM (PCFM) Radar Waveforms, Part I: Implementation," *IEEE Transactions on Aerospace and Electronic Systems*, vol. 50, no. 3, pp. 2218–2229, 2014.
[10] S. D. Blunt, J. Jakabosky, M. Cook, J. Stiles, S. Seguin, and E. L. Mokole, "Polyphase-Coded FM (PCFM) Radar Waveforms, Part II: Optimization," *IEEE Transactions on Aerospace and Electronic Systems*, vol. 50, no. 3, pp. 2230–2241, 2014.
[11] K. Alhujaili, X. Yu, G. Cui, and V. Monga, "Spectrally Compatible MIMO Radar Beampattern Design Under Constant Modulus Constraints," *IEEE Transactions on Aerospace and Electronic Systems*, vol. 56, no. 6, pp. 4749–4766, 2020.
[12] M. Wicks, "Spectrum Crowding and Cognitive Radar," in *2010 2nd International Workshop on Cognitive Information Processing*, 2010, pp. 452–457.
[13] A. Farina, A. De Maio, and S. Haykin, *The Impact of Cognition on Radar Technology*, ser. Radar, Sonar and Navigation. Institution of Engineering and Technology, 2017.
[14] J. Guerci, *Cognitive Radar: The Knowledge-Aided Fully Adaptive Approach, Second Edition*. Artech House, US, 2020.
[15] S. Haykin, "Cognitive Radar: A way of the Future," *IEEE Signal Processing Magazine*, vol. 23, no. 1, pp. 30–40, 2006.
[16] R. Klemm, U. Nickel, C. Gierull, P. Lombardo, H. Griffiths, and W. Koch, *Novel Radar Techniques and Applications Volume 2: Waveform Diversity and Cognitive Radar, and Target Tracking and Data Fusion*, ser. Radar, Sonar & Navigation. Institution of Engineering and Technology, 2017.
[17] M. S. Greco, F. Gini, P. Stinco, and K. Bell, "Cognitive Radars: On the Road to Reality: Progress Thus Far and Possibilities for the Future," *IEEE Signal Processing Magazine*, vol. 35, no. 4, pp. 112–125, 2018.
[18] S. Z. Gurbuz, H. D. Griffiths, A. Charlish, M. Rangaswamy, M. S. Greco, and K. Bell, "An Overview of Cognitive Radar: Past, Present, and Future," *IEEE Aerospace and Electronic Systems Magazine*, vol. 34, no. 12, pp. 6–18, 2019.
[19] M. A. Govoni, "Enhancing Spectrum Coexistence using Radar Waveform Diversity," in *2016 IEEE Radar Conference (RadarConf)*, 2016, pp. 1–5.
[20] H. He, P. Stoica, and J. Li, "Waveform Design with Stopband and Correlation Constraints for Cognitive Radar," in *2010 2nd International Workshop on Cognitive Information Processing*, 2010, pp. 344–349.
[21] Y. Huang, M. Piezzo, V. Carotenuto, and A. De Maio, "Radar Waveform Design under Similarity, Bandwidth Priority, and Spectral Coexistence Constraints," in *2017 IEEE Radar Conference (RadarConf)*, 2017, pp. 1142–1147.
[22] A. Martone, K. Sherbondy, K. Ranney, and T. Dogaru, "Passive Sensing for Adaptable Radar Bandwidth," in *2015 IEEE Radar Conference (RadarCon)*, 2015, pp. 0280–0285.
[23] A. F. Martone, K. I. Ranney, K. Sherbondy, K. A. Gallagher, and S. D. Blunt, "Spectrum Allocation for Noncooperative Radar Coexistence," *IEEE Transactions on Aerospace and Electronic Systems*, vol. 54, no. 1, pp. 90–105, 2018.
[24] J. A. Kovarskiy, J. W. Owen, R. M. Narayanan, S. D. Blunt, A. F. Martone, and K. D. Sherbondy, "Spectral Prediction and Notching of RF Emitters for Cognitive Radar Coexistence," in *2020 IEEE International Radar Conference (RADAR)*, 2020, pp. 61–66.
[25] A. Aubry, V. Carotenuto, A. De Maio, and M. A. Govoni, "Multi-Snapshot Spectrum Sensing for Cognitive Radar via Block-Sparsity Exploitation," *IEEE Transactions on Signal Processing*, vol. 67, no. 6, pp. 1396–1406, 2019.
[26] S. Blunt and E. Perrins, *Radar and Communication Spectrum Sharing*, ser. Radar, Sonar and Navigation. Institution of Engineering and Technology, 2018.
[27] V. Carotenuto, A. Aubry, A. De Maio, N. Pasquino, and A. Farina, "Assessing Agile Spectrum Management for Cognitive Radar on Measured Data," *IEEE Aerospace and Electronic Systems Magazine*, vol. 35, no. 6, pp. 20–32, 2020.
[28] A. Aubry, V. Carotenuto, A. De Maio, A. Farina, A. Izzo, and R. Schiano Lo Moriello, "Assessing power amplifier impairments and digital predistortion on radar waveforms for spectral coexistence," *IEEE Transactions on Aerospace and Electronic Systems*, vol. 58, no. 1, pp. 635–650, 2022.
[29] O. A. Krasnov, L. P. Ligthart, Z. Li, P. Lys, and F. van der Zwan, "The parsax - full polarimetric fmcw radar with dual-orthogonal signals," in *2008 European Radar Conference*, 2008, pp. 84–87.
[30] Z. Wang, O. A. Krasnov, G. P. Babur, L. P. Ligthart, and F. van der Zwan, "Reconfigurable digital receiver for polarimetric radar with dual-orthogonal signals," in *The 7th European Radar Conference*, 2010, pp. 332–335.
[31] O. A. Krasnov, G. P. Babur, Z. Wang, L. P. Ligthart, and F. van der Zwan, "Basics and first experiments demonstrating isolation improvements in the agile polarimetric fm-cw radar parsax," *International Journal of Microwave and Wireless Technologies*, vol. 2, no. 3-4, p. 419428, 2010.